

## The Dynamics of the Hydride Ion in MgO Single Crystals

M.A.Monge<sup>1</sup>, R.González<sup>1</sup>, A.I.Popov<sup>1,3</sup>, R.Pareja<sup>1</sup>,  
Y.Chen<sup>2</sup>, E.A.Kotomin<sup>3,4</sup> and M.M.Kuklja<sup>5</sup>

<sup>1</sup> Departamento de Física, Escuela Politécnica Superior, Universidad Carlos III,  
Avda. de la Universidad, 30, 28911 Leganés, Madrid, Spain

<sup>2</sup> Division of Materials Sciences, Department of Energy, Germantown, MD 20874-1290, USA

<sup>3</sup> Institute for Solid State Physics, University of Latvia, 8 Kengaraga, LV-1063 Riga, Latvia

<sup>4</sup> Fachbereich Physik, Universität Osnabrück, D-49069, Germany

<sup>5</sup> Department of Electrical Engineering, Michigan Technological University,  
Houghton, MI 49931, USA

**Keywords:** MgO, Diffusion, H<sup>-</sup>, Activation energy, Hartree-Fock

**Abstract.** Diffusion of H<sup>-</sup> ions in thermochemically reduced MgO crystals with a large concentration of hydrogen has been investigated both experimentally and theoretically. Infrared absorption of the [H<sup>-</sup>]<sup>+</sup> centers is used to monitor the concentration and to study their diffusion rates in crystals heated at elevated temperatures in flowing oxygen. Characteristic parameters such as activation energy and diffusion coefficients were determined. The diffusion coefficient is  $\approx 10^{-6}$  cm<sup>2</sup>/s at 1600 K. The activation energy is estimated experimentally to be  $(1.5 \pm 0.3)$  eV. Analysis of the decay curves of [H<sup>-</sup>]<sup>+</sup> center concentrations during isothermal anneals indicates that the annealing-out of the [H<sup>-</sup>]<sup>+</sup> centers does not follow a first-order kinetic reaction. The H<sup>-</sup> ion diffusion was simulated using an *ab-initio* Hartree-Fock cluster approach. The mobile defect is more compatible with the H<sup>-</sup> ion than with the proton. Theoretical modeling for the direct interstitial H<sup>-</sup> hops along the [100] axis gives an activation energy twice as large as the experimental value. It is proposed that either a collinear interstitialcy mechanism for diffusion, or motion of the H<sup>-</sup>-oxygen vacancy complex are involved.

### 1 Introduction

Hydrogen is an impurity that affects the optical and electronic properties of many oxide materials [1-23]. In general, all oxide crystals contain hydrogen to a greater or lesser extent. In particular, in MgO crystals, hydrogen appears primarily in three basic forms or configurations: H<sub>2</sub>, OH<sup>-</sup> and H<sup>-</sup> ions; the source of hydrogen is moisture absorbed by MgO powder prior to crystal growth. The first form is high-pressure hydrogen gas (H<sub>2</sub>) present in cavities which result in opacity of the crystals [24, 25]. The second configuration is hydroxyl ions (OH<sup>-</sup>) in isolated or in Mg(OH)<sub>2</sub> precipitate form. The single OH<sup>-</sup> radicals substitute directly for O<sup>2-</sup> ions. Since OH<sup>-</sup> is deficient in negative charge relative to O<sup>2-</sup>, charge compensation is necessary. Thus, an hydroxyl ion occupying an anion site is charge compensated by a neighboring cation vacancy. The complex with the linear configuration of OH<sup>-</sup>[++]<sup>2-</sup>, where [++] refers to a magnesium vacancy, is commonly referred to as V<sub>OH</sub><sup>-</sup>. This defect has a stretching vibration mode that results [26, 27] in optical absorption at 3296 cm<sup>-1</sup>. At elevated temperatures, there is an equilibrium between protons at V<sub>OH</sub><sup>-</sup> sites and in Mg(OH)<sub>2</sub> precipitates. The latter are characterized by a band at 3700 cm<sup>-1</sup>. Lastly, an H<sup>-</sup> substituting for an O<sup>2-</sup> ion can only be produced after very severe thermochemical reduction (TCR)[3, 6].

Studies of hydrogen substituting for oxygen in thermochemically reduced MgO crystals have shown fascinating optical properties [3-12]. Thermochemical reduction, which is a

very strong reduction process, leads to a stoichiometric deficiency of oxygen ions, resulting in oxygen vacancies. These vacancies are usually occupied by two electrons (F center) and are therefore electrically neutral [3, 6]. At high temperatures protons can be trapped by these vacancies, forming  $[H^-]^+$  centers [3, 6, 11, 28, 29]. This notation follows that prescribed by Sonder and Sibley [30]. Hereafter, we will distinguish between the  $[H^-]^+$  center (a proton with two electrons in an  $O^{2-}$  vacancy and the  $H^-$  ion (a proton with two electrons in an interstitial position). The cavities containing high-pressure  $H_2$  gas serve as a perpetual source of hydrogen during high-temperature treatments.

$[H^-]^+$  centers have been identified by local vibrational modes at 1053, 1032 and 1024  $cm^{-1}$  (see Refs. 3 and 6). Attempts to observe the optical absorption induced by the electronic transitions of the  $[H^-]^+$  centers in the wide energy range of 0.5 – 6 eV were unsuccessful [12]. This failure will be discussed theoretically.

$[H^-]^+$  centers play an important role in the F center long-lived luminescence through electron trapping by  $[H^-]^+$  centers, resulting in the formation of  $[H^{2-}]^0$  centers [11, 12]. The presence of the  $[H^{2-}]^0$  center has been verified by EPR spectroscopy of deuterium-enriched MgO crystals [7].

Previous studies indicate that  $[H^-]^+$  centers are thermally more stable than F centers when heated either in oxygen or in a reducing atmosphere.  $[H^-]^+$  centers can survive annealing in a reducing atmosphere at temperatures as high as 1900 K without loss in concentration [6]. This indicates that the presence of a proton in an oxygen vacancy stabilizes the vacancy against thermal annihilation.

In the past two decades much effort has been devoted to studying proton diffusion in prospective ceramics (see [15, 16] and references therein). One of the motivations for these studies was the potential use of ceramics for hydrogen-storage applications due to their low permeability to hydrogen. Hydrogen diffuses more slowly into ceramics than into metals [31]. The solubility of  $H^+$  or  $D^+$  in oxides is low even at high temperatures. The maximum concentration of these isotopes in oxides is of the order of  $10^{18} cm^{-3}$ . Also the diffusion coefficients at high temperatures are very low compared to those in metals [4, 25]. Unlike metals, refractory oxides can withstand high temperatures and effectively serve as barriers to permeability of hydrogen and its isotopes [4, 25]. In spite of this effort, the mechanisms for hydrogen diffusion in ceramics are in general unknown.

In the present paper, we have studied both theoretically and experimentally the diffusion characteristics of  $H^-$  ions in hydrogen-doped MgO crystals after TCR. Parameters such as diffusion coefficients and activation energies were determined.

## 2 Experimental procedure

The MgO crystals used in the present investigation were grown [32] by the arc-fusion method at the Oak Ridge National Laboratory using high-purity-grade MgO powder from the Kanto Chemical Company, Tokyo, Japan. Crystals with a high concentration of hydrogen were obtained by presoaking MgO powder with  $H_2O$ . As-grown crystals were thermochemically reduced in a tantalum chamber containing high pressure of magnesium vapor by heating at  $\approx 2000$  K and then fast cooled.

Optical absorption measurements in the far infrared were made with a Perkin-Elmer 2000 FT-IR spectrophotometer. Heat treatments were made either in flowing oxygen or inside a graphite container inserted in a horizontal furnace with flowing oxygen-free nitrogen gas.

## 3 Experimental results

### 3.1 Mathematical formalism

The diffusion characteristics for a classical system with a low concentration of defects or impurities such that they do not interact with each other can be described by Fick's second

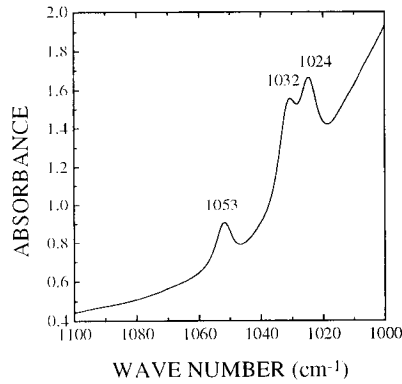


**Fig. 1.** Infrared absorption spectrum for  $[H^-]^+$  centers in a thermochemically reduced MgO crystal.

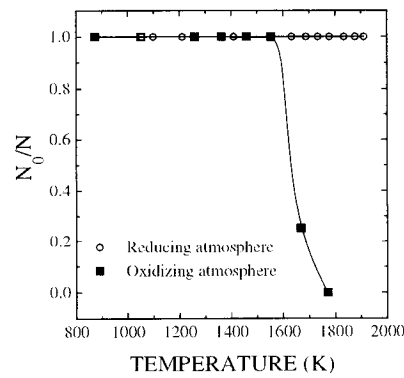


**Fig. 2.** Normalized concentration *vs* isochronal annealing temperature of two thermochemically reduced MgO samples in: (a) reducing atmosphere, (b) flowing oxygen.

law; in an isotropic medium the rate of transfer of the diffusing species through a unit area of a section is proportional to the concentration gradient measured perpendicular to the section [20, 33]. In one dimension, Fick's second law can be written as

$$\frac{\partial C}{\partial t} = D \frac{\partial^2 C}{\partial x^2} \quad (1)$$

where  $C$  is the concentration of the diffusing species,  $x$  is the coordinate along the axis perpendicular to the surface, and  $D$  is the diffusion coefficient. For dilute systems,  $D$  can be considered independent of  $C$ . At time  $t$  the total concentration of the diffusing species in a sample of thickness  $2d$  is given by

$$C(t) = \frac{1}{2d} \int_{-d}^d C(x, t) dx \quad (2)$$

where  $C(x, t)$  is the *local* concentration of the diffusing species at annealing time  $t$ . Here we are interested in the  $H^-$  ion diffusion out of a plane sheet of area  $S$  and thickness  $2d$ , through which the diffusing substance is initially uniformly distributed, and the surfaces of which are kept at zero concentrations. Let  $C_0$  be the initial concentration (at  $t = 0$ ) of the diffusing species in the sample and  $C(x, t)$  be that at annealing time  $t$ . The diffusion equation [20, 33], is as follows:

$$C(x, t) = \frac{4C_0}{\pi} \sum_{n=0}^{\infty} \frac{(-1)^n}{2n+1} \exp\left(-\frac{D_{out}(2n+1)^2\pi^2 t}{4d^2}\right) \times \cos\left(\frac{2n+1}{2d}\pi x\right). \quad (3)$$

Integration of Eq. 2 yields

$$C(t) = \frac{8C_0}{\pi^2} \sum_{n=0}^{\infty} \frac{1}{(2n+1)^2} \exp\left(-\frac{D_{out}(2n+1)^2\pi^2 t}{4d^2}\right). \quad (4)$$

$C(t)$  in Eq. 4 is proportional to the optical absorbance  $A(t)$  of the  $H^-$  ions in the crystal. Retaining the first term of Eq. 4, the out-diffusion coefficients can be calculated from the slope  $M$  of a semi-logarithmic plot of the absorbance after annealing for the time  $t$ ,  $A(t)$ ,

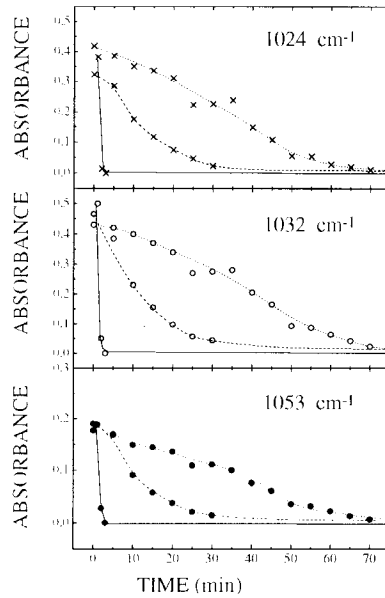


**Fig. 3.** Absorbance of the  $[H^-]^+$  bands at 1024, ( $\times$ ), 1032 ( $\circ$ ), and 1053  $\text{cm}^{-1}$  ( $\bullet$ ) against annealing time for three samples annealed in flowing oxygen at 1530 (dot line), 1630 (dashed line) and 1750 K (solid line).

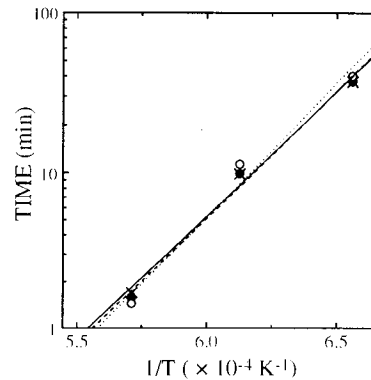


**Fig. 4.** Log of the times for the three crystals to reach the same arbitrary absorbance values at 1024, 1032 and 1053  $\text{cm}^{-1}$  vs the reciprocal of the annealing temperature.

against isothermal annealing time using the expression

$$D_{out} = \frac{4Md^2}{\pi^2} \quad (5)$$

### 3.2 Diffusion measurements

Fig. 1 depicts the infrared spectrum showing three  $[H^-]^+$  local modes at 1024, 1032 and 1053  $\text{cm}^{-1}$  in a TCR MgO crystal. The presence of three sharp, closely spaced bands (none intensity correlated) indicates that they are of different species, presumably with different impurity compensators [6]. The thermal stability of  $[H^-]^+$  centers was determined by subjecting two TCR crystals to isochronal anneals of 10 min duration in either reducing or oxidizing atmospheres. The initial  $[H^-]^+$  concentration of these crystals was estimated [6] to be  $\approx 2.9 \times 10^{18} \text{ cm}^{-3}$ . The results are plotted in Fig. 2.

The annihilation depends on the atmosphere. In oxygen, all the  $[H^-]^+$  vanished by 1800 K. In a reducing atmosphere, the concentration remained unchanged even at 1923 K. In agreement with previous findings, all three  $[H^-]^+$  bands decrease at the same rate.

In order to determine the activation energy and diffusion coefficients, isothermal annealing of 5 min duration in flowing oxygen at 1530, 1630 and 1750 K was performed on three crystals with the same thickness ( $\approx 1.5 \text{ mm}$ ) and the same initial  $[H^-]^+$  concentration. After each anneal, the absorbances of the corresponding  $[H^-]^+$  band were measured. Fig. 3 illustrates the decay of the three  $[H^-]^+$  bands at each temperature. The activation energy for the annealing-out of  $[H^-]^+$  centers was obtained using the cross-cut method [34]. In Fig. 4 the times for the three crystals to reach the same arbitrary absorbance value are plotted against the reciprocal to the annealing temperature  $1/T$ . The activation energies

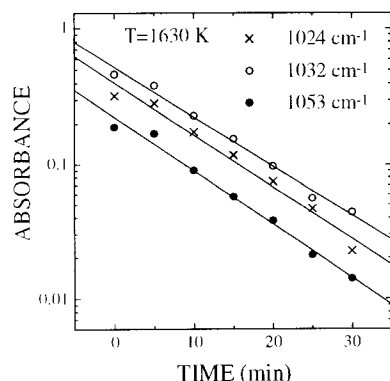


Fig. 5. Log of the absorbance of the  $[H^-]^+$  bands vs isothermal annealing time at 1630 K.

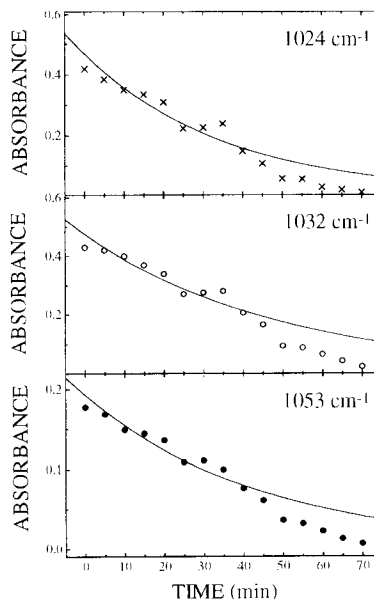


Fig. 6. IR absorbances of the  $[H^-]^+$  bands vs isothermal annealing time at 1530 K. The solid lines represents the best fit of the experimental data to a single exponential.

for the three bands are found to be:  $E(1024 \text{ cm}^{-1}) = (1.4 \pm 0.2)$ ,  $E(1032 \text{ cm}^{-1}) = (1.5 \pm 0.3)$ , and  $E(1053 \text{ cm}^{-1}) = (1.4 \pm 0.2)$  eV, respectively.

Assuming that  $[H^-]^+$  centers are annealed-out at the surface of the crystal, a semilogarithmic plot of the  $[H^-]^+$  absorbances versus isothermal annealing time for the three temperatures yields, using Eq. 5, the out-diffusion coefficients (Fig. 5). The corresponding values are summarized in Table I. It is of interest to compare the out-diffusion coefficients of hydrogen from  $[H^-]^+$  centers with the diffusion coefficients for the exchange of  $H^+$  for  $D^+$  in  $V_{OH}^-$  centers. In the latter, the diffusion coefficient [4] is of the order of  $10^{-6} \text{ cm}^2/\text{s}$  at 1873 K.

The decay curves of the  $[H^-]^+$  center concentrations during isothermal anneals at 1530, 1630 and 1750 K can only be poorly fitted to a single exponential (see Fig. 6), which indicates that the annealing of the  $[H^-]^+$  centers does not occur by a first order reaction.

Table 1. Experimentally estimated diffusion coefficients of  $[H^-]^+$  centers in MgO.

Temperature (K)	Out-diffusion coefficients for the three $[H^-]^+$ bands ( $\times 10^{-6} \text{ cm}^2/\text{s}$ )			Mean Value
	1024 $\text{cm}^{-1}$	1032 $\text{cm}^{-1}$	1053 $\text{cm}^{-1}$	
1530	$(0.9 \pm 0.4)$	$(0.7 \pm 0.3)$	$(0.8 \pm 0.3)$	$(0.8 \pm 0.3)$
1630	$(1.5 \pm 0.6)$	$(1.4 \pm 0.6)$	$(1.5 \pm 0.6)$	$(1.5 \pm 0.6)$
1750	$(500 \pm 200)$	$(380 \pm 150)$	$(320 \pm 140)$	$(400 \pm 160)$

## 4 Theoretical

### 4.1 Calculation method

In the simulations of the  $[H^-]^+$  centers, we have used the embedded molecular cluster model combined with *ab initio* molecular orbital theory based on the *Hartree-Fock* (HF) formalism. Our method is similar to the DICAP code which was found very useful in studies of defects in alkali halides [35]. Our approach and its application to defects in MgO are described in detail in Ref. [36]. For calculations of the static (both atomic and electronic) properties of the  $[H^-]^+$  center, a 27-atom quantum cluster  $[Mg_{12}O_{14}H]^{-1}$  of  $O_h$  symmetry was used in *ab initio* calculations. This cubic-shaped cluster consists of a single, negatively charged  $[H^-]^+$  defect in its center and three spheres of surrounding ions. The wave function for the excited state of the  $[H^-]^+$  center is expected to be rather diffuse (similar to the  $[H^{2-}]^0$  center [37]). This is in agreement with the experimental fact that the ground state energy level of the  $[H^{2-}]^0$  center lies close to the bottom of the conduction band; the same is to be expected for the  $[H^-]^+$  excited state. Therefore we have augmented the standard 31 G basis set for the  $[H^-]^+$  center with an additional diffuse orbital with an exponent of 0.08 a.u. Six nearest neighbor (NN)  $Mg^{2+}$  cations and another eight  $Mg^{2+}$  cations from the third sphere were treated in the valence approximation using the 21/21 G basis set [38]. Their cores were represented by effective core pseudopotentials [39]. Twelve  $O^{2-}$  anions, which are the 2NNs of the defect, were considered as all-electron atoms with 721/41 G basis set [38]. The Madelung potential of the crystalline lattice field was simulated by 200 point charges surrounding the quantum cluster. To improve the cluster boundary conditions,  $Mg^{2+}$  ions nearest to the cluster were simulated by bare core pseudopotentials without basis functions attached. In order to allow geometric optimization for ions in a quantum cluster, short-range interactions between  $O^{2-}$  ions outside the cluster and  $Mg^{2+}$  ions inside the cluster have been described by atom-atom potentials (see more in [35, 36]):

$$\phi_{ij}(r_{ij}) = A_{ij} \exp(-r_{ij}/\rho_{ij}) \quad . \quad (6)$$

The parameters of these potentials ( $A_{ij} = 46.8624$  a.u. and  $\rho_{ij} = 1.7569$  a.u.) were taken from Ref. [40].

The total energy gradient optimization technique was employed to search for the equilibrium ground-state configuration of the cluster. In *ab initio* studies we used the Gaussian-92 computer code [38]. This code was modified to include classical contributions (Eq. 6) to the total energy, energy gradients [35] and energy derivatives for the cluster in the field of point charges [36].

The same method was also applied in defect diffusion simulations using 81-atom quantum clusters (see below). In these calculations we have optimized the equilibrium and saddle point geometry for the jumping interstitial  $H^-$  ion at the beginning and in the middle of its path, respectively. The activation energy for a diffusion jump is the difference between the corresponding total energies, calculated for the relaxed lattice around the defect.

### 4.2 Theoretical results

The optimized ionic displacements for the three NN spheres of ions and the effective charges on the ions surrounding the  $[H^-]^+$  center are given in Table 2. In our *ab initio* calculations, the  $Mg^{2+}$  ions are displaced outwards from the defect by 1 % of the Mg-O distance due to the Coulomb repulsion from the positively charged  $[H^-]^+$  center. The 2NN  $O^{2-}$  ions are displaced inwards by 4 %. Similar  $O^{2-}$  ion displacements but larger  $Mg^{2+}$  displacements were obtained in previous *ab initio* ICECAP calculations [37].

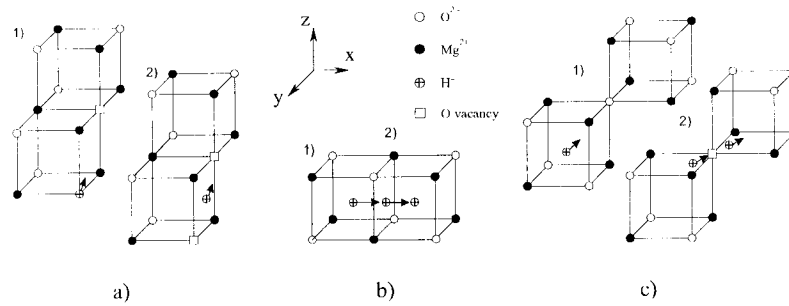


**Fig. 5.** a) Vacancy mechanism of the substitutional  $[H^-]^+$  center diffusion: 1) the initial (ground) state, 2) the saddle point. b) Direct jump of the  $H^-$  interstitial through the cube face during its  $[100]$  hop. c) Collinear interstitialcy mechanism of the  $H^-$  ion diffusion; 1) the initial state, 2) the saddle point.

**Table 2.** Results of *ab initio* calculations of the ionic displacements (in units of the interatomic Mg–O distance,  $a_0 = 2.1$  Å) and effective charges (in  $|e|$ ) on ions surrounding the  $[H^-]^+$  center in the substitutional position in MgO crystals.

Atom	Coordinates of atom			Charge on atom
	$x$	$y$	$z$	
<i>ab initio</i> , present study				
H	0.00	0.00	0.00	-0.458
Mg	1.01	0.00	0.00	1.608
O	0.97	0.97	0.00	-1.803
Mg	1.00	1.00	1.00	1.899
<i>ab initio</i> , ICECAP [37]				
Mg	1.03	0.00	0.00	-
O	0.97	0.97	0.00	-
Mg	1.03	1.03	1.03	-

The effective charges of  $Mg^{2+}$  and  $O^{2-}$  ions are close to those expected for purely ionic bonding ( $\pm 2e$ ) (according to the Mulliken population analysis). Our calculations predict half an electron of the  $[H^-]^+$  center to be delocalized, mainly over the NN  $Mg^{2+}$  ions.

As follows from our calculations, the  $[H^-]^+$  center has two local states. One of them, occupied by two electrons, lies *below* the bottom of the O  $2p$  upper valence band, with the energy separation about 1 eV. Another empty energy level is 7 eV above the top of the valence band. These results are in qualitative agreement with those obtained in the Local Density Approximation (LDA) calculations [41]. The fact that a virtual state (vacant energy level) of the  $[H^-]^+$  center lies very close to the bottom of the conduction

**Table 3.** Atomic displacements (in units of  $a_0=2.1$  Å) and charges on ions (in  $|e|$ ) around  $H^-$  ions in MgO during its diffusion hop along the  $[100]$  axis obtained in the *ab initio* HF calculation (Fig. 7.b).

Center-of-cube configuration				Saddle point configuration					
Atom	Coordinates			Charge on ion	Atom	Coordinates			Charge on ion
	$x$	$y$	$z$			$x$	$y$	$z$	
H	0.50	0.00	0.00	-0.352	H	0.00	0.00	0.00	-0.431
Mg	0.02	0.46	0.46	1.607	Mg	0.00	0.51	0.51	1.746
O	-0.07	0.54	-0.54	-1.745	O	0.00	0.61	-0.61	-1.714
Mg	0.95	-0.45	0.45	1.640	Mg	0.92	-0.47	0.47	1.701
O	1.04	0.54	0.54	-1.834	O	0.99	0.50	0.50	-1.859
Mg	-0.98	-0.48	0.48	1.843	Mg	-0.92	-0.47	0.47	1.701
O	-1.00	0.49	0.48	-1.834	O	-0.99	0.50	0.50	-1.859

band makes this center a shallow trap for electrons. Thus, the  $[H^-]^+$  center ion acts as an efficient trap for electrons released from the F centers, as discussed in Ref. [12].

As a result, the optical absorption energy for the  $[H^-]^+$  center is estimated to be around 10 eV, far inside the absorption edge of MgO (7.8 eV). This explains why the electronic transition of the  $[H^-]^+$  center has not been observed in the region of 0.5 – 6.0 eV (see more details in Ref. [42]).

We now discuss possible mechanisms for the *diffusion* of the  $[H^-]^+$  center in MgO. At the onset, the question arises as to what species is responsible for the mobility of the  $[H^-]^+$  center. Is it due to protons hopping from F centers to F centers or due to diffusion of the  $H^-$  ion as a whole? Calculations in conjunction with the experimental results will show that the mobile defect is not the proton; therefore we consider the  $H^-$  ion as the mobile species. In principle, the  $[H^-]^+$  center can exchange its position with an  $O^{2-}$  (*the vacancy mechanism*), or the  $H^-$  ion becomes an interstitial. If it goes to the interstitial position, there are again two possibilities: to make direct hops along the  $[100]$  axis (*direct interstitialcy mechanism*), or along the  $[111]$  axis via the so-called *collinear interstitialcy mechanism*. All three mechanisms are shown schematically in Fig. 7. Using the *ab initio* HF method, we modeled the first two mechanisms. We found that a standard vacancy mechanism (Fig. 7.a) is not energetically feasible since the exchange of positions between an  $[H^-]^+$  center and an  $O^{2-}$  vacancy requires a very large activation energy due to the mutual repulsion of these two positively charged defects. This is in agreement with the high activation energy value (4.85 eV) found for  $H^-$  diffusion for this mechanism using the shell-model [37].

Next we assume that a substitutional  $H^-$  ion leaves the  $O^{2-}$  vacancy to an interstitial position and then moves through the crystal as an interstitial (Fig. 7.b). We have simulated the  $H^-$  ion diffusion by such a direct interstitialcy mechanism using the above described *ab initio* HF method. The  $[Mg_{40}O_{40}H]^-$  cluster employed in these *ab initio* calculations contained two adjacent cubes. The basis set was placed on 13 central atoms, and the other atoms were represented by pseudopotentials. The quantum cluster was embedded in the crystal field modeled by 172 point charges. Twelve atoms nearest to the defect were allowed to relax.

In the equilibrium interstitial configuration, the  $H^-$  ion is situated in an interstitial position



in the cube center, then it hops along the [100] axis (Fig. 7.b) with the saddle point at the cube face.

The effective ionic charges and displacements are summarized in Table 3. Calculations clearly show that in both equilibrium and saddle points the defect has an effective charge between a neutral atom,  $H^0$ , and a single-charged  $H^-$  ion, but is unlikely to be a proton. The largest displacements correspond to NN  $O^{2-}$  ions due to the Coulomb repulsion with the  $H^-$  ion. Our calculations show that such direct interstitial jumps require an activation energy of  $\approx 3$  eV. However, the experimental results presented in section 3.2 yield an activation energy of  $\approx 1.5$  eV for the annealing-out of the  $[H^-]^+$  centers. To resolve this discrepancy, it is of interest to simulate the collinear interstitialcy mechanism for the  $H^-$  ion diffusion (Fig. 7.c) where an interstitial  $H^-$  ion moves from the center of the cube along the [111] body diagonal and in its saddle point forms a dumbbell with an  $O^{2-}$  ion. Recent shell-model calculations for self-interstitials ( $Mg^{2+}$ ,  $O^{2-}$ ) in MgO show that the activation energy for collinear interstitial diffusion could be about half of that for direct interstitial jumps [43].

Yet another possibility is that the  $H^-$  ion and its oxygen vacancy moves as a complex, periodically associating and dissociating. The activation energies for the hopping of this complex may be smaller than those for the two individual defects. Due to the Coulomb attraction to the  $H^-$  ions, the oxygen vacancies do not anneal as isolated F centers. It is very difficult to model this mechanism theoretically; at the moment we can only say that the jump of the  $H^-$  ion from the substitutional to the interstitial position requires an activation energy larger than that for the isolated  $H^-$  ion diffusion.

## 5 Summary and conclusions

IR absorption bands at 1053, 1032, and 1024  $cm^{-1}$ , due to the local vibrational modes of the  $[H^-]^+$  centers, were used to monitor their concentration in hydrogen-laden MgO crystals after TCR. Three crystals were subjected to isothermal anneals in flowing oxygen at 1530, 1630, and 1750 K, respectively. Based on the decay curves for the  $[H^-]^+$  concentrations, using the cross-cut method [34], an activation energy of  $\approx 1.5$  eV was obtained. Assuming that  $[H^-]^+$  centers diffused to the crystal surface during the heat treatments at elevated temperatures, the out-diffusion coefficients were determined. At 1600 K, the resulting value is  $\approx 10^{-6}$   $cm^2/s$ . Analysis of the decay curves indicates that the  $[H^-]^+$  centers do not anneal-out following a first order reaction.

The  $[H^-]^+$  center diffusion was simulated using an *ab-initio* Hartree-Fock cluster approach. The mobile defect is more compatible with the  $H^-$  ion than with the proton. Two possible mechanisms were modeled. First, a *standard vacancy* mechanism (the  $[H^-]^+$  center exchanges with an  $O^{2-}$  vacancy) was found to be not energetically feasible since that position exchange requires a very large activation energy. Second, a *direct interstitialcy* mechanism requires that the  $H^-$  ion leaves its oxygen vacancy, becomes an interstitial, and subsequently hops along the [100] axis. This mechanism yields an activation energy of  $\approx 3$  eV, twice that measured experimentally. We suggest that a *collinear interstitialcy* mechanism (the interstitial hydride ion hops along the [111] axis and in its saddle point forms a dumbbell with an  $O^{2-}$  ion in a regular site) could provide an activation energy closer to the experimental value. However, for an asymmetric  $H^- - O^{2-}$  dumbbell, it is not easy to optimize the defect geometry at the saddle point. Alternatively, the motion of the  $H^-$ -oxygen vacancy complex is also considered. This correlated motion can be characterized by the activation energy which is likely smaller than those for the individual defects.

## 6 Acknowledgments

Research at the University Carlos III was supported by the Comisión Interministerial de Ciencia y Tecnología (CICYT) of Spain. The research of Y.C. is an outgrowth of past investigations performed at the Oak Ridge National Laboratory. A.I.P. was supported by the Latvian Research Council (grant No 96.0666) and E.A.K. by the Deutsche Forschungsgemeinschaft through the grant to the Osnabrück University. A. I. P. also acknowledges the Dirección General de Enseñanza Superior e Investigación Científica of Spain for support. Authors are indebted to prof. S. Kapphan for valuable discussions.

## References

- [1] W. Hayes and A. M. Stoneham, *Defects and Defect-Induced Processes in Non-Metallic Solids* (Wiley, 1985).
- [2] J. M. Cabrera, J. Olivares, M. Carrascosa, J. Rams, R. Muller, and E. Diéguez, *Adv. in Physics*, **45**, 349 (1996).
- [3] R. González, Y. Chen, and M. Mostoller, *Phys. Rev. B* **24**, 2682 (1981).
- [4] R. González, Y. Chen, and K. L. Tsang, *Phys. Rev. B* **26**, 4637 (1982).
- [5] G. P. Summers, T. M. Wilson, B. T. Jeffries, H. T. Tolver, Y. Chen, and M. M. Abraham, *Phys. Rev. B* **27**, 1283 (1983).
- [6] Y. Chen, R. González, O. E. Schow, and G. P. Summers, *Phys. Rev. B* **27**, 1276 (1983).
- [7] J. Tombrello, H. T. Tolver, Y. Chen, and T. M. Wilson, *Phys. Rev. B* **30**, 7374 (1984).
- [8] Y. Chen and R. González, *Optics Lett.* **10**, 276 (1985).
- [9] R. González and Y. Chen, *Phys. Rev. B* **35**, 206 (1987).
- [10] Y. Chen, V. M. Orera, and G. J. Pogatschnik, *Phys. Rev. B* **42**, 1410 (1990).
- [11] V. M. Orera and Y. Chen, *Phys. Rev. B* **36** 1244 (1987); *Phys. Rev. B* **36**, 6120 (1987).
- [12] Y. Chen, R. González, V. M. Orera, and G. J. Pogatschnik, *Disordered Systems and new Materials*, World Scientific, pp.96-112 (1989).
- [13] V. M. Orera, M. L. Sanjuan, and Y. Chen, *Phys. Rev. B* **42**, 7604 (1991).
- [14] S. C. Ke, D. C. Patton, J. G. Harrison, and H. T. Tolver, *J. Phys.: Condens. Matter.* **7**, 9625 (1995).
- [15] R. Ramírez, R. González, I. Colera, and R. Vila, *J. Amer. Ceram. Soc.* **80**, 847 (1997).
- [16] R. Ramírez, R. González, I. Colera, and Y. Chen, *Phys. Rev. B* **55**, 237 (1997).
- [17] R. González, Y. Chen, J. F. Barhorst, and K. L. Tsang, *J. Mat. Res.* **2**, 77 (1987).
- [18] Y. Chen, R. González, and K. L. Tsang, *Phys. Rev. Lett.* **53**, 1077 (1984).
- [19] R. González, E. R. Hodgson, C. Ballesteros, and Y. Chen, *Phys. Rev. Lett.* **67**, 2057 (1991).
- [20] R. González, C. Ballesteros, Y. Chen, and M. M. Abraham, *Phys. Rev. B* **39**, 11085 (1989).
- [21] R. González, R. Hantelzadeh, C. Y. Chen, L. E. Halliburton, and Y. Chen, *Phys. Rev. B* **39**, 1302 (1989).
- [22] K. O. Kreuer, *Chem. Mater.* **8**, 610 (1996).
- [23] S. Kapphan and A. Breitzkopf, *Phys. Stat. Solidi A* **133**, 159 (1992); A. Förster, H. Hesse, S. Kapphan, and M. Wöhlecke, *Solid State Comm.*, **57**, 373 (1986); K. Buse, S. Breer, K. Peithmann, S. Kapphan, M. Gao, and E. Krätzig, *Phys. Rev. B* **56**, 1225 (1997); A. Gröme and S. Kapphan, *J. Phys.: Cond. Matter*, **7**, 3051; 6393 (1995).
- [24] A. Briggs, *J. Mater. Sci.* **10**, 729 (1975).
- [25] M. S. Corisco, R. González, and C. Ballesteros, *Phil. Mag.* **52**, 699 (1985).
- [26] P. Kirklin, P. Auzins, and J. E. Wertz, *J. Phys. Chem. Solids* **26**, 1667 (1965).

- [27] B. Henderson and W. A. Sibley, *J. Chem. Phys.* **55**, 1276 (1971).
- [28] J. T. Gourley and E. R. Vance, *Phys. Status Solidi B* **77**, K85 (1976).
- [29] E. R. Vance and W. C. Mallard, *Phys. Status Solidi B* **91**, K155 (1979).
- [30] E. Sonder and W. A. Sibley, in *Point Defects in Solids*, edited by J. H. Crawford, Jr. and L. Slifkin (Plenum, New York, 1972). Likewise the  $H^{-2}$  ion in an oxygen vacancy can also be denoted  $[H^{2-}]^0$ .
- [31] J. Volkl and G. Alefeld, in *Hydrogen in Metals I*, ed. by G. Alefeld and J. Volkl (Springer, Berlin) (1978).
- [32] M. M. Abraham, C. T. Butler, and Y. Chen, *J. Chem. Phys.* **55**, 3752 (1971).
- [33] J. Crank, *The Mathematics of Diffusion*, 2<sup>nd</sup> ed. (Clarendon, Oxford) (1975).
- [34] A. C. Damask and G. J. Dines, *Point Defects in Metals* (Gordon and Breach, New York, 1963).
- [35] V. E. Puchin and N. Itoh, *Phys. Rev. B* **52**, 6254 (1995); V. E. Puchin, A. L. Shluger, and N. Itoh, *Phys. Rev. B* **52**, 6254 (1995); V. E. Puchin, A. L. Shluger, K. Tanimura, and N. Itoh, *Phys. Rev. B* **47**, 6226 (1993).
- [36] M. A. Johnson, E. V. Stefanovich, and T. N. Truong, *J. Phys. Chem. B* **101**, 3196 (1997).
- [37] R. Pandey and J. M. Vail, *J. Phys. C.: Condens. Matter* **1**, 2801 (1989); J. M. Vail, *J. Phys. Chem. Solids* **51**, 589 (1990).
- [38] M. J. Frisch, G. W. Trucks, M. Head-Gordon, P. M. W. Gill, M. W. Wong, J. B. Foresman, B. G. Johnson, H. B. Schlegel, M. A. Robb, E. S. Replogle, R. Gomperts, J. L. Andres, K. Raghavachari, J. S. Binkley, C. González, R. L. Martin, D. J. Fox, D. J. Defres, J. Barker, J. J. P. Stewart, and A. Pople, *GAUSSIAN 92 Users Guide*, Gaussian Inc. Pittsburg, PA, (1992).
- [39] W. R. Wadt and P. J. Hay, *J. Chem. Phys.* **82**, 284 (1985).
- [40] R. Pandey, J. Zuo, and A. B. Kunz, *J. Mater. Res.* **5**, 623 (1990).
- [41] Q. S. Wang and N. A. W. Holzwarth, *Phys. Rev. B* **41**, 3211 (1990).
- [42] M. M. Kuklja, E. V. Stefanovich, E. A. Kotomin, A. I. Popov, R. González, and Y. Chen, *Phys. Rev. B*, **59**, 1885 (1999).
- [43] E. A. Kotomin, P. W. M. Jacobs, N. E. Christensen, T. Brudevoll, M. M. Kuklja, and A. I. Popov, *Defect and Diffusion Forum*, **143-147**, 1231 (1997).

This article was processed using the L<sup>A</sup>T<sub>E</sub>X macro package with TTP style

